Research Square

Preprints are preliminary reports that have not undergone peer review.
They should not be considered conclusive, used to inform clinical practice,
or referenced by the media as validated information.

Escalating habitat warming in Amazonian rivers shifting turtle hatchlings sex-ratios towards feminization

Shirley Famelli

shifacbio@yahoo.com.br

University of Bristol https://orcid.org/0000-0001-9790-4986

Ayan Fleischmann

Instituto de Desenvolvimento Sustentável Mamirauá

Gustavo Willy Nagel

University of Southampton

Roberto Victor Lacava

Brazilian Institute of Environment and Renewable Natural Resources

Evlyn Marcia Leão de Moraes Novo

National Institute for Space Research

Filipe Machado França

University of Bristol

Priscila Saikoski Miorando

Federal University of Western Pará

Paulo Cesar Machado Andrade

Federal University of Amazonas

Camila R. Ferrara

Wildlife Conservation Society

Palmira Francisca Gonçalves Ferreira

SEMAS Pará

Fernanda P. Werneck

National Institute of Amazonian Research

Diogo Lima Franco

Instituto de Desenvolvimento Sustentável Mamirauá

Raphael Alves Fonseca

Brazilian Institute of Environment and Renewable Natural Resources

Rodolfo L. B. Nóbrega

University of Bristol

Research Article

Keywords: climate change ecology, ectotherms, freshwater ecology, hydrology, temperature dependent sex-determination

Posted Date: November 6th, 2026

DOI: https://doi.org/10.21203/rs.3.rs-11460215/v1

License: This work is licensed under a Creative Commons Attribution 4.0 International License. Read Full License

Additional Declarations: The authors declare no competing interests.

Escalating habitat warming in Amazonian rivers shifting turtle hatchlings sex-ratios towards feminization

Shirley Famelli[1]✉, Ayan Fleischmann[2], Gustavo Willy Nagel[3], Roberto Victor Lacava[4,5], Evlyn Marcia Leão de Moraes Novo[6], Filipe França[7], Priscila Saikoski Miorando[8], Paulo Cesar Machado Andrade[9], Camila R. Ferrara[10], Palmira Francisca Gonçalves Ferreira[11], Fernanda P. Werneck[12], Diogo Lima Franco[2], Raphael Alves Fonseca[4], Rodolfo L. B. Nóbrega[1]

[1] University of Bristol, Faculty of Science, School of Geographical Sciences, Bristol, United Kingdom of Great Britain-England, Scotland, Wales.

[2] Mamirauá Institute for Sustainable Development, Tefé, Amazonas, Brazil

[3] School of Geography and Environmental Sciences, University of Southampton, Southampton, SO17 1BJ, UK

[4] Instituto Brasileiro do Meio Ambiente e Recursos Naturais Renováveis (IBAMA), Avenida Tapajós, nº 2.267, Bairro Laguinho, Postal Code 68010-000, Santarém, Pará, Brazil.

[5] Universidade Federal do Oeste do Pará (UFOPA), Rede Bionorte - Postgraduate Program in Biodiversity and Biotechnology, Pará, Brazil.

[6] Earth Observation and Geoinformatics Division, National Institute for Space Research, SP, Brazil

[7] University of Bristol, Faculty of Science, School of Biological Sciences, Bristol, United Kingdom of Great Britain-England, Scotland, Wales.

[8] Universidade Federal do Oeste do Pará (UFOPA), Instituto de Formação Interdisciplinar e Intercultural, Pará, Brazil.

[9] Universidade Federal do Amazonas (UFAM), Faculdade de Ciências Agrárias, Departamento de Produção Animal e Vegetal, Laboratório de Animais Silvestres, Programa Pé-de-pincha, Manaus, AM, Brazil.

[10] Wildlife Conservation Society-WCS Brasil, Manaus, AM, Brazil.

[11] Secretaria de Estado de Meio Ambiente, Clima e Sustentabilidade do Pará, Pará, Brazil.

[12] Coordenação de Biodiversidade, Programa de Coleções Científicas Biológicas, Instituto Nacional de Pesquisas da Amazônia – INPA, Manaus, Brazil.

✉E-mail: s.famelli@bristol.ac.uk

Abstract

Amazonia is experiencing more frequent and severe weather extremes. Freshwater species, like the endangered Giant Amazonian turtles, *Podocnemis expansa,* are key for assessing how climate change influences Amazonian rivers and biodiversity. Extreme habitat temperatures can increase turtle embryo mortality; however, other non-lethal effects are expected due to their temperature-dependent sex determination, which can eventually drive populations to become predominantly female-biased. Using in-situ and satellite-based data from 1998 to 2024, we show escalating warming trends, up to +0.3ºC a year, in the water and sandbanks of three major Amazon Basin rivers (Purus, Trombetas, and Tapajós) used by turtles for nesting. We then estimated the sex-ratio of all hatchlings bourn at these sandbanks monitored by local communities. We observed that, as warming intensifies, cohorts unlikely reach balanced sex-ratios, with the magnitude of the bias progressively shifting towards more females, while males comprise less than 15% of offspring. Our results emphasize the need for long-term nest-temperature observations and monitoring as a critical conservation effort to access ongoing population changes under future warming scenarios.

Introduction

Climate change is reshaping ecosystems globally, with unforeseen consequences for aquatic wildlife. Rapid warming represents an urgent threat to freshwater ecosystems, which is believed to be especially challenging in the tropics, where species can be more sensitive to temperature changes due to narrower thermal niches[1]. Among tropical freshwater systems, the Amazon Basin stands out as particularly important because of its ecological complexity coupled with the accelerating pace of environmental change, making it a unique natural setting for studying the implications of temperature changes to biodiversity, enabling novel satellite-based retrievals and analytical methods[2]. The Amazon River encompasses some of the planet's most extensive aquatic ecosystems, contributing to approximately 15–20% of the world's freshwater flow into the oceans[2]. These waters govern and nurture exceptional terrestrial and freshwater biodiversity associated with its flood pulses and ecological annual cycles, that also form the basis for the subsistence, mobility, and socio-cultural practices of local riverine communities along these rivers[3–5].

During regular annual flooding cycles, as water levels recede, riverbanks become progressively exposed, reaching their maximum extent in the dry season, when large sandbars form along the rivers, until the onset of the wet season, which submerges them again[2]. These sandbanks serve as rich nurseries grounds for several species, attracting an array of predators and key species for ecosystem functioning and socio-ecological services[6]. Still, changes in river dynamics associated with extreme flooding and droughts, are becoming more intense, driven by a warmer, longer and drier dry season, with insidious hydro-social-ecological consequences[7,8]. Alterations in the hydrological regime, such as decreasing low flows associated with droughts, can subsequently reduce thermal buffering and lead to more rapid warming of freshwater systems[2,9]. The Amazon River and its tributaries generally present river temperatures within 1-2 degrees of 29ºC[7]. Yet, in 2023 and 2024, Amazonia experienced its most severe recorded droughts, drastically impacting local communities, hydroelectric production, water supply, and unexpected biodiversity losses[10–12]. Over Amazonian lakes, elevated water temperatures reaching up to 41ºC led to mass mortality of river dolphins, and major fish kill events were recorded across the basin[13,14].

Most freshwater organisms are ectothermic, and their reliance on environmental temperature and consequent inability to use metabolic heat to maintain body temperature, place them at high risk to the current climate crisis[1,14,15]. Freshwater reptiles are especially vulnerable, as they often rely on both terrestrial and aquatic habitats and are subject to escalating, interconnected threats impacting both habitats[16]. Amazonian river turtles, like the Giant Amazonian turtles, *Podocnemis expansa*, are naturally connected to the annual river flood pulses[16,17], and alterations in these dynamics can affect the suitability of nesting sites and shift their breeding timing, later impacting their reproductive success[16,17].

As long-lived animals, turtles are critical wildlife for investigating the potential long-term impacts of rising river temperatures on Amazonian biodiversity. Most turtle species exhibit temperature-dependent sex determination (TSD)[18,19], with higher temperatures tending to favour the development of more females than males in Amazonian species[19]. Hence, all hatchlings may develop as males at lower incubation temperature (full masculinizing), or 100% females at high temperatures (full feminizing)[20], except when reaching extreme and lethal temperatures (below 28°C and above 40°C for the *P. expansa*). The pivotal temperature (Tpiv), which produces a 1:1 (female:male) sex-ratio, for *P. expansa* is 32.6°C[19], with possible geographical

variation. With temperatures below 28°C lethal for embryos[19], the species' full masculinizing shows a very restricted range around 29.5°C[19]. Amazonian turtles' hatchlings show no evident external sexual dimorphism[21,22]. Thus, invasive techniques must be applied to differentiate males to females, such as (a) the animals to be dissected in a laboratory and the sexual organs prepared histologically[21,22]; (b) the determination of testosterone seric level after Follicle-Stimulating Hormone (FSH) injection method[20,22]; or (c) laparoscopy[22]. Although a recent blood-based method has made it possible to determine the sex of individual turtle hatchlings[23], estimating sex-ratios at the scale of entire nesting sites or populations remains challenging. With such harmful or expensive techniques, limited field long-term observations are currently available regarding temperature-driven sex-ratio bias in wild populations. This knowledge gap hinders our ability to predict whether climate-induced shifts in sex-ratios will translate into long-term population declines, altering species interactions and reducing ecosystem functions supported by turtles, such as seed dispersal, nutrient cycling, and the maintenance of Amazonian floodplain ecosystems. Here we present a method to understand these relationships, combining in-situ water temperature from three Amazonian rivers (Purus, Trombetas, and Tapajós), Landsat thermal infrared (TIR) images to explore long-term changes of river water and land (sandbanks) temperature, and information on nesting for the Giant Amazonian turtle monitored by local communities in partnership with the Brazilian Government. Based on the number of hatchlings born in each of these monitored nesting refuges and the incubation temperatures predicted on the satellite scenes, we estimated the sex-ratio of hatchlings. We then discuss the implications of habitat warming and temperature changes over 26 years for Amazonian turtles' sex-ratio fluctuations, examining responses in relation to climate-driven variability. Predicted sex-ratios were consistently female-biased for all regions throughout the years. Yet, as warming intensifies, the magnitude of the bias progressively shifts towards a greater proportion of females with males' numbers dropping lower than 10% in hot years. Recovery toward more balanced sex-ratios is unlikely without the occurrence of substantially cooler years.

Turtles nesting refuges in Amazonia

The study areas were selected considering their importance for turtles and because they contain long, continuous datasets on turtle hatchling from at least 1998 to 2024: (A) Purus River: a highly meandering lowland river, characterized by its sinuosity,

and one of the main right-bank tributaries of the Amazon River. At Purus, we investigated changes within the Abufari Biological Reserve (REBio Abufari), Amazonas State, with relative stability in turtle hatchlings numbers[24]; another in the (B) Trombetas River: a clearwater tributary of the Amazon River, within the Trombetas River Biological Reserve (ReBio Trombetas), Pará State, showing decline on turtle hatchlings along the years; and at (C) Tapajós River: a clear to white water river which supports immense biodiversity and many traditional and indigenous communities, while facing high anthropogenic pressures. Monte Cristo is a beach located outside a protected reserve monitored by IBAMA, near the Tapajós-Amazon confluence, in the proximities of Santarém. At Monte Cristo the number of hatchlings has been increasing along the years (Fig. 1).

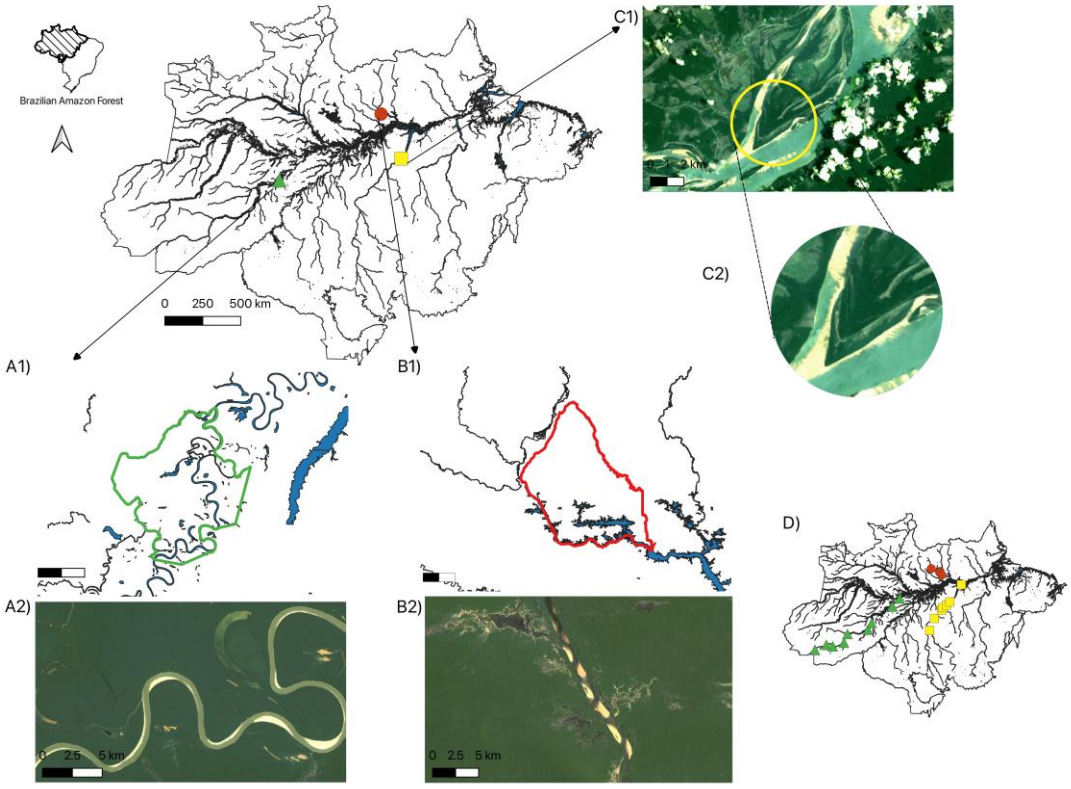


Fig. 1. Study areas across the Brazilian Amazon. (A1) Abufari Biological Reserve in the Purus River (green triangle); (B1) Trombetas Biological Reserve in the Trombetas River (red dot), and (C1) Sandbanks in Tapajós River, monitored by IBAMA (yellow square). Satellite images (A2, B2, C1) show the region of interest in each study area. (C2) shows the region with available in-situ sand temperature collected with dataloggers within the Monte Cristo sandbar (2018, 2019, and 2024). (D) Shows the distribution of the gauges with in-situ water temperature data.

Increased water temperature over Amazonian rivers

Apart from for Trombetas River (TR), we observed increasing trends in median water temperature over the years in all datasets used to investigate temporal changes in water temperature: Brazilian Hidroweb (collected in-situ) and Landsat (satellite observations using random points within the region of interest – ROI), and Water Surface Temperature (WST) using all available masked pixels in the Landsat scene (see methods). The trends in the in-situ temperature data varied across the seasons, method, and study site (Fig. 2 and 3). At Purus (PU) and Tapajós (TJ), the trends were moderate ($\tau = 0.281$, $p = 0.04$) and strong ($\tau = 0.457$, $p =< 0.001$), respectively. At Purus, satellite temperatures were consistently higher than in-situ by an average of 2–3°C (paired t-test, $p < 0.01$ for all windows $\geq \pm 3$ days). At Purus, across all datasets, Sen's slope ranged +0.05 to 0.23°C per year. At Trombetas, Sen's slope estimates varied from +0.07 to 0.13°C per year. On the other hand, at Tapajós the increase in Sen's slope ranged from of +0.16 to 0.18°C a year (Table 1; Fig. 3). The temperatures between the datasets were moderately correlated when observations matched within ±3 days ($r = 0.656$) and ±5 days ($r = 0.579$). At Tapajós, satellite temperatures were consistently lower than in-situ, with mean differences ranging from 0.7 to −1.5°C. At Trombetas, satellite temperatures were also lower by approximately 1–2°C with increasing trends only in WST data ($\tau = 0.299$, $p < 0.05$; Table 1). In all areas, the WST shows a shift towards warmer conditions over time, with increasing dominance of the 30–35°C class and a growing contribution of higher temperature ranges (35–40°C), alongside a decline in cooler classes (15–25°C). A chi-square test indicated that temperatures differed significantly among year–month combinations (Table 2). The strength of this association was low to moderate depending on the region (TR: Cramér's $V = 0.284$; TJ: $V = 0.341$; PU: $V = 0.499$), suggesting uneven representation of months across years (Fig. 3 and 4).

Increasing sand temperatures

Sand/Land Surface Temperature (LST) varied markedly among years in all areas and were unevenly distributed, indicating that some temperature ranges occurred more frequently than others (Table 2; Fig. 4). The effect size was small to moderate (TJ: Cramér's $V = 0.26$; TR: Cramér's $V = 0.39$; PU: Cramér's $V = 0.49$), depending on the study site. October and November, the peak of the dry season, were the warmest

months across multiple years in all study areas (Fig. 4; Supplementary Fig. 1). However, at Purus, from 2022, extreme temperatures began to occur earlier in September, while November showed occasional peaks, particularly in 2023. At Purus, larger exposed sand areas were associated with higher temperature. For every 1 km² increase in sand area, median sand temperature increases by ~1°C ($p = 0.006$). Sand area explained approximately 10% of the variation in temperature at Purus ($R^2 = 0.10$) (Fig. 5). However, this relation was not observed at Trombetas (Pearson's $r \approx 0.02$, $p < 0.001$; $R^2 \approx 0.0003$), nor at Tapajós (Pearson's $r = 0.107$, $p = 0.359$; $R^2 = 0.012$) (Supplementary Fig. 2 and 3).

At Trombetas, most observations were concentrated in the warm to very hot ranges, indicating limited occurrence of cooler microhabitats in this region. At Tapajós, low temperatures (28–38°C) were dominant at the beginning of the timeseries. However, temperatures ≥40°C progressively became more frequent from 2012 onwards. A Mann–Kendall test indicated a significant increasing trend in median temperature over time in all areas (PU: $\tau = 0.275$, $p = 0.05$; TR: $\tau = 0.16$, $p = 0.0096$; TJ: $\tau = 0.286$, $p = 0.043$). Sen's slope estimated a median increase of +0.3°C per year at Purus; +0.04°C per year at Trombetas; and +0.12°C per year at Tapajós (Table 1; Fig. 4).

At Tapajós, nesting incubation temperature collected using dataloggers during the 2018, 2019, and 2024 indicated a progressive increase across the monitored years. Despite the small sample size, 2024 exhibited the highest incubation temperatures, with median of 33.4°C (30.5–38.26°C), followed by 2019 with median of 32°C (29–32.2°C), while 2018 experienced the coolest conditions with median of 31.5°C (27.5–36.5°C). Agreement between satellite sand temperatures and in-situ temperatures improved as the temporal matching window decreased (Pearson $r = 0.53$), while Root Mean Square Error (RMSE) decreased from 3.71°C to 2.92°C. These results indicate that temporal mismatch contributes substantially to disagreement between methods, although satellite temperatures remained consistently warmer than datalogger measurements by approximately 2–4°C. Restricting the Landsat-derived temperature extraction to the area immediately surrounding the datalogger locations improved agreement between satellite and in-situ measurements. Pearson correlation increased from $r = 0.27$ to $r = 0.38$, while the proportion of explained variance doubled ($R^2 = 0.07$ to 0.14). This improvement suggests that the spatial mismatch between satellite data and datalogger locations contributed substantially to the discrepancies observed

in the broader-scale analysis. Landsat-derived sand temperatures exhibited a stronger relationship with Early Morning datalogger measurements (r = 0.43, RMSE = 3.35°C) than with Morning measurements (r = 0.34, RMSE = 3.64°C). In both cases, satellite temperatures were consistently higher than in situ temperatures, with mean differences ranging from 2.7 to 3.7°C. This pattern suggests that satellite-derived temperatures capture broad thermal variation observed in the field but remain influenced by differences in measurement scale and timing. Since dataloggers were available only at Tapajós, the uncertainty associated with satellite-estimates may be greater in the other two study areas. The comparison between in-situ sand temperature and satellite-estimated was used as a base for a sensitivity analysis on hatchlings sex-ratios.

Hatchlings sex-ratios following high sand temperatures

Prediction on sex-ratios based on the LST showed a tendency in favour of females for all regions throughout the years. The data indicate persistent female dominance in warm years, with substantial interannual variation, with males eventually shifting the magnitude of the bias or even outnumbering females in the occurrence of cooler years. Following the sensitivity analysis, the predicted sex-ratios remained female-biased across most years and scenarios, although the magnitude of the female bias generally declined from Scenario1 (original satellite data) to Scenario4 (-4°C; Fig 6). Overall, Scenario4 predicted fewer females than Scenario1, on average it was 8.89 (TR), 16.37 (PU), and 25.2 (TJ) percentage points in each site, with an equivalent increase in the predicted male proportion. Nevertheless, more balanced sex-ratio were predicted in the first 10 years of the timeseries in all areas and scenarios in comparison to the last half of the timeseries. Under the intermediate scenario (Scenario3: -3°C), at Purus, females represented between 27.1% and 94.9% of the predicted population, exceeding 70% in most years. Male representation was particularly low in several years, falling below 15% when sand temperature was high (Fig. 4 and 6). At Trombetas, females comprised between 39.4% and 95.8% of the predicted population along the years. In some years, males represented less than 8% of individuals. In 2022, male representation increased sharply to 60.6%, producing the most balanced sex-ratio at this site since 2014. At Tapajós, female proportions ranged from 27.8% and 87.3% of the predicted population. Sex-ratios were relatively

balanced in 1999 and 2006, whereas in 2010 males predominated, accounting for 53.8% of the predicted population at this site. Following this temporary shift, female-biased sex-ratios resumed and persisted through 2024, suggesting long-term dominance of female production despite substantial interannual variability (Fig. 7; Supplementary Fig. 4 and 5). The sex-ratio estimation based on the dataloggers distributed at Tapajós was also female-biased, except in 2024, when, although the temperatures were extremely high, the predictions flipped to males. According to Hill's equation, it was predicted 73.6% females in 2018, 58.1% in 2019, and 39.6% in 2024 with 60.4% males (Fig. 8).

Ecological implications of extreme temperatures for Amazonian turtles

Our data demonstrated an increasing trend in the habitat temperature, aggravated by extreme events. Intense droughts caused habitat temperatures to increase both in water and on land (sandbanks), with Amazonian water temperatures that typically range from 25 to 30°C, progressively concentrated in the upper end of the range. High water temperatures have been registered in Amazonian lakes even at depth, meaning limited thermal refuge for aquatic wildlife[13].

Chelonians (turtles and tortoises) managed to survive over 200 million years of natural selection and long-term environmental pressures and challenges[25], however, some of their life-history traits have turned into disadvantages amid extreme changes of the Anthropocene[25]. Climate change represents a multiple-stressors challenge, altering complex abiotic factors with effects ranging from adult reproductive physiology to embryonic development[22]. Thermal preferences and thermoregulatory regimes are poorly understood for most turtles, especially in tropical environments[1]. The combined increase in temperatures on land and in water means that these and other animals could face challenges cooling down under very high, even lethal, temperatures[1].

While heat-mediated conditions are expected to increase turtle embryos mortality, other non-lethal effects on reproduction may also drive populations toward vulnerability and consequent decline as a response to climate change[20,23]. Heat stress can affect food availability for reproductive females, altering their physiology, nesting

phenology, resource allocation to the eggs, as well as the habitat where embryonic development takes place[20,23]. Warmer habitats can, thereby, potentially disturb the gonadal cycles of turtles, which can determine the first day of nesting for a population[20]. In Amazonia, turtles' nesting cycles are synchronised with the water cycles and exposure of sandbanks. *Podocnemis expansa*, one of the most social turtle species worldwide[26], exhibits a complex coordinated mass nesting known as *arribada*, in which females aggregate on sandbanks during the dry season to synchronize egg-laying[26]. A consequence of this behaviour is that clutches may experience similar comparable incubation conditions resulting in similar sex-ratios[20]. Under warming conditions, future cohorts are unlikely to maintain balanced sex-ratios, with populations becoming progressively more female-skewed over time. Our estimates indicate that males may represent less than 15% of offspring, highlighting the potential for severe demographic consequences in populations with temperature-dependent sex determination (TSD). These findings have important conservation implications, suggesting that continued warming may drive demographic changes that threaten the long-term persistence of TSD populations.

Sex-ratio estimations were female-skewed in the three study areas, linked to incubation temperatures predicted in those environments, with a tendency for more males to be produced under wetter/cooler conditions, and more females under drier/hotter environments[20]. In general, the proportions of male hatchlings to female hatchlings in *P. expansa* favours females in 1:30 (1 male to 30 females)[21]. Although responses differed geographically, it was more intense in the second half of our timeseries with increasing thermal trends, which suggests that embryos may suffer from development abnormalities, lethal temperatures or, owing to temperature-sex determination (TSD) features in turtles, those able to survive could be developed mostly as females, potentially leading to a feminization of the next generations, unless cooler years occur to rebalance the bias. However, our time series indicate that cooler years are becoming increasingly rare. Having their population sex-ratio tied to an environmental variable represents an evolutive disadvantage that can lead to changes in population sizes, long-term viability, and consequent extinction[20]. As global warming sex-ratio imbalances threaten a wide range of taxonomically diverse TSD groups, early detection of declining male abundance is of critical conservation

importance, as their rarity compromises the future of reproduction and the viability of populations[27].

It is known that females do not nest at random with turtles selecting nesting sites that differ in their characteristics, being vegetation cover, soil moisture, texture, or distance to the water[16,20]. Thus, the nesting site choice and its features can influence incubation temperature and humidity, which, in turn, determine subsequent developmental phases, growth rate, offspring size, number, survival, the sex of embryos, and, consequently, reproductive success[20]. Moreover, nests temperature may be much cooler in the shade, yet, sandbanks are not typically vegetated, with most nests laid in the open, sunny parts of the beach[19]. Shaded and vegetated nests do not conform to the typical natural incubation for Amazonian turtle species nests, except *Podocnemis unifilis* that additionally to the sandbanks, nests at vegetated riverbanks[28]. Shaded nests appear to face high mortality rates, as temperatures can be too low for embryos development[19,20]. Furthermore, nests' distance from the water can influence the moisture in its chamber, which varies with the rising and falling water tables and with precipitation events[20]. Moisture can help insulate the soil against rapid air temperature fluctuations[20]. Conversely, heated water may pose a risk to nests near the river margin as they may experience increased thermal exposure. Observations from local communities indicate the presence of undeveloped eggs in all study sites, likely due to high temperatures that have led to embryonic mortality.

Incubation temperature may likewise differ within a single egg chamber, varying between the upper and the bottom eggs, contributing to the reduction of the occurrence of unisexual clutches[19,20]. Shallow, more superficial nests, generally laid by smaller females, are more prone to being affect by extreme temperatures fluctuations than deeper nests, built by larger females, which are commonly cooler[19, 20]. Under cooler temperatures, deeper nests tend to produce a higher percentage of male hatchlings in comparison to shallow nests[19]. Females should bury deeper nests as they grow, thus, young females may produce more daughters and older females producing more sons[19,20]. Still, numerous threats faced by turtles mean little chance of growth, with large adult females becoming rarer in the wild as they are also heavily targeted for human consumption. Therefore, satellite-derived temperatures capture broad thermal variation observed in the field but remain influenced by differences in

measurement scale and timing. All these variabilities can explain the discrepancies of 2 to 4°C between satellite-derived and in-situ sand temperature, which in addition, can be affected by moisture, shading, vegetation, solar radiation, or even sand colour. Although the uncertainty caused by these differences may be addressed by our sensitivity analysis, predictions were still female-biased in all scenarios. This underscores the need for in-situ monitoring to validate temperature estimates, track changes in sex-ratios, and guide management strategies that promote long-term population resilience and viability amid extreme temperatures. Nevertheless, extremely fluctuations in mean nest temperatures may also reverse offspring sex-ratio, resulting in a marked predominance of males[29], apart from high rates of mortality, slower developmental rates, and much smaller sizes[29,30]. This scenario, although rare, appears to have occurred in our sex-ratio estimation for the dataloggers in 2024. It has also been reported in isolated field observations in 2023 in Amazonia[28]. However, further research is needed to determine the conditions under which this response occurs.

Amazonia satellite imagery can be highly affected by clouds. Temperature varies on rainy, cooler days and amid sun and wind exposure, not captured by satellite imagery, as cloud shadows undermine confidence in the results[31]. Nevertheless, clouds attenuate incoming shortwave radiation, leading to cooler surface conditions. Therefore, years with no imagery available were perhaps cooler and could be more fitting to produce more males. Thus, variations in weather conditions between nesting seasons can mitigate the effects of anomalously hot or wet years over the long term[38]. Again, our data shows that the pronounced thermal anomalies caused by subsequently extreme events may alter the annual capacity of wildlife to recover following uncharacteristic climatic oscillations.

As water temperatures rose, the sandbanks temperatures also increased in all study areas. Water temperature is an easily monitored variable that can trigger timely action when needed. On the other hand, substrate type, mineral composition, and granule size can also affect moisture and thermal energy absorption, and therefore, the incubation conditions[20]. Soil thermal uptake is further influenced by solar radiation, air temperature, and precipitation[20], which vary daily, seasonally, and geographically. Given the geographic and geological heterogeneity of Amazonia, increases in water

temperature vary spatially and is likely river-specific, with a mosaic of complex effects and patterns[4,32,33], with some rivers more resilient to change than others[33]. Trombetas, a clear-water river, did not show increasing trends, however, this site showed high temperatures from the beginning of the series in comparison to Purus and Tapajós. Early studies at Trombetas revealed a tendency to produce a higher proportion of female[21]. Thus, it is expected that population structure, incubation, pivotal temperature, and sex-ratios will vary across the species' extensive and heterogeneous geographic distribution[19,22]. Consequently, some populations might be more likely to withstand thermal stress.

Extreme droughts and floods in Amazonia are expected to be more frequent, with projections that Amazonian waters will get hotter, more acidic (lower pH), carbonated (higher CO_2), and hypoxic (lower O_2)[2,32], with ample implications for wildlife. Thermal pollution can impact fecundity and fertility across a broad taxonomic range, with varied physiological, morphological, and evolutionary responses[34]. Though the consequences of extreme heat on reproductive outputs may vary among individuals and species, reproduction is a primary biological feature for population stability and persistence through the recruitment of new individuals, especially for animals with late sexual maturity and long generations. While female-biased sex-ratios may be more advantageous, since relatively few males can fertilize many females[18]. Sex-ratios bias is generally considered a threat, and little is known regarding the consequences of persistent hatchling female bias along the years, which may ultimately compromise population viability, especially in already endangered species. Currently, there is no evidence that Amazonian turtles can adapt to a rising global temperature scenario, nor that females adjust nesting site selection to improve hatchling survival[20]. Despite this, some species demonstrate behavioural or physiological plasticity, potentially buffering the impacts of future climatic and environmental change[20]. The Amazonian turtles constitute an important economic and cultural resource for indigenous and traditional communities inhabiting its distributional range across Amazonia. The continuous investment in the Amazonian Turtles Conservation Program is imperative for the survival of these animals. Their protection can yield co-benefits for diverse taxa, from aquatic to terrestrial species, as well as for the communities that depend on these ecosystems. In the face of a changing climate, integrating our findings into target nesting monitoring frameworks

can inform the development of adaptative management and policies to mitigate mortality and sex-ratio bias (e.g. dataloggers; potentially nest shading and refuge for adults).

References

1. Kidman, R. A., Mcknight, D. T., Schwarzkopf, L. & Nordberg, E. J. Too cold is better than too hot : Preferred temperatures and basking behaviour in a tropical freshwater turtle. 1532–1546 (2023) doi:10.1111/aec.13335.
2. Fassoni-Andrade, A. C. *et al.* Amazon Hydrology From Space: Scientific Advances and Future Challenges. *Rev. Geophys.* **59**, 1–97 (2021).
3. Vasconcellos, A. M. de A. & Vasconcellos Sobrinho, M. The meanings of rural community according to nature of community livelihood in Brazilian Amazonia. *Interações (Campo Gd.* 21–30 (2017) doi:10.20435/inter.v18i2.1545.
4. Andrade, P. C. M. *et al.* Community-Based Conservation and Management of Chelonians in the Amazon. *Front. Ecol. Evol.* **10**, (2022).
5. Campos-Silva, J. V, Hawes, J. E., Andrade, P. C. M. & Peres, C. A. Unintended multispecies co-benefits of an Amazonian community-based conservation programme. *Nat. Sustain.* **1**, 650–656 (2018).
6. Andrade, P.C.M. Azevedo, S.H. Duarte, J.A.M. Garcez, J.R. Oliveira, P.H.G. Pinto, J.R.S. Almeida Jr., C. D. P. *Projeto Pé-de-Pincha: Técnicas de Conservação e Manejo de Quelônios - Manual Do Monitor de Praia*. (2015).
7. Marengo, J. A. *et al.* The Drought of Amazonia in 2023-2024. 567–597 (2024) doi:10.4236/ajcc.2024.133026.
8. Padilha, J. *et al.* Worsening Drought and the Bleak Future for Biodiversity and Ecosystem Services in the Amazon Basin. *Aquat. Conserv. Mar. Freshw. Ecosyst.* **35**, e70101 (2025).
9. White, J. C., Malcolm, I. A., Krause, S. & Hannah, D. M. Drought impacts on river water temperature : A process-based understanding from temperate climates. 1–21 (2023) doi:10.1002/hyp.14958.
10. Lindsey, R. Climate.gov: Science and Information for a Climate-Smart Nation. National Oceanic and Atmospheric Administration (NOAA). *Drought parches the central Amazon in October 2023* https://www.climate.gov/news-

features/event-tracker/drought-parches-central-amazon-october-2023 (2023).

11. Santos de Lima, L., Magalhães de Oliveira, H. F., Fleischmann, A. S. & Macedo, M. N. Extreme drought is again isolating people in Amazonia. *Nature* **622**, 697–697 (2023).
12. Marmontel, M., Fleischmann, A., Val, A. & Forsberg, B. Safeguard Amazon's aquatic fauna against climate change. *Nature* **625**, 450–450 (2024).
13. Fleischmann, A. S. *et al.* Extreme warming of Amazon waters in a changing climate. 606–611 (2025).
14. Braz-Mota, S. & Val, A. L. Fish mortality in the Amazonian drought of 2023 : the role of experimental biology in our response to climate change. *J. Exp. Biol.* **227**, jeb247255 (2024).
15. Stocker, C. *et al.* Temperature variability does not influence phenotypic plasticity in ectotherms – a meta-analysis. 1–15 (2025).
16. Eisemberg, C. C. *et al.* Vulnerability of giant South American turtle (*Podocnemis expansa*) nesting habitat to climate-change-induced alterations to fluvial cycles. *Tropical Conservation Science.* **9**, (2016).
17. Do Vale, R., Filizola, N., Souza, R. & Schongart, J. The flood of 2009 in the Brazilian Amazon. *Rev. Bras. Geociencias* **41**, 577–586 (2011).
18. Laloë, JO., Cozens, J., Renom, B. et al. Effects of rising temperature on the viability of an important sea turtle rookery. Nature Climate Change 4, 513–518 (2014).
19. Valenzuela, N. Constant, shift, and natural temperature effects on sex determination in Podocnemis Expansa turtles. *Ecology* **82**, 3010–3024 (2001).
20. Topping, N. E. & Valenzuela, N. Turtle Nest-Site Choice , Anthropogenic Challenges , and Evolutionary Potential for Adaptation. **9**, 1–12 (2021).
21. Camillo, C. S., Valenzuela, N. & Johnson, S. A. Effects of semi-constant temperature on embryonic and hatchling phenotypes of six-tubercled Amazon River turtles , Podocnemis sextuberculata. *J. Therm. Biol.* **108**, 103292 (2022).
22. Bonach, K., Malvasio, A., Matushima, E. R. & Verdade, L. M. Temperature-sex determination in Podocnemis expansa (Testudines, Podocnemididae). *Iheringia - Ser. Zool.* **101**, 151–155 (2011).
23. Tezak, B., Sifuentes-Romero, I., Milton, S. et al. Identifying Sex of Neonate Turtles with Temperature-dependent Sex Determination via Small Blood Samples. *Sci Rep* **10**, 5012 (2020).

24. Forero-Medina, G. *et al.* On the future of the giant South American river turtle *Podocnemis expansa*. *Oryx* 1–8 (2019) doi:10.1017/S0030605318001370.
25. Chen, C., Wang, J., Holyoak, M. et al. Global assessment of current extinction risks and future challenges for turtles and tortoises. *Nature Communication*. **16**, 7114 (2025).
26. Souza, M. M. de *et al.* Movement and habitat use of female subadults of Podocnemis expansa (Testudines: Podocnemididae) in northern Brazil. *Phyllomedusa Journal of Herpetology.* **24**, 25–44 (2025).
27. Hays, G. C., Laloë, J.-O., Lee, P. L. M. & Schofield, G. Evidence of adult male scarcity associated with female-skewed offspring sex ratios in sea turtles. *Curr. Biol.* **33**, R14–R15 (2023).
28. Brito, E. S. *et al. Quelônios Continentais e Crocodilianos Do Brasil*. (Agência Estadual de Meio Ambiente do Estado de Pernambuco, Recife, 2025).
29. Neuwald, J.L. & Valenzuela, N. The Lesser Known Challenge of Climate Change: Thermal Variance and Sex-Reversal in Vertebrates with Temperature-Dependent Sex Determination. PLoS ONE 6(3): e18117 (2011).
30. Magalhães, M.S., Vogt, R.C., Sebben, A. et al. Embryonic development of the Giant South American River Turtle, *Podocnemis expansa* (Testudines: Podocnemididae). Zoomorphology 136, 523–537 (2017).
31. Meng, X. *et al.* Accuracy Evaluation of the Landsat 9 Land Surface Temperature Product. **15**, 8694–8703 (2022).
32. Val, A. L. & Wood, C. M. Global change and physiological challenges for fish of the Amazon today and in the near future. *J Exp Biol*. **15**;225(10):jeb216440 (2022).
33. Johnson, M. F. *et al.* Rising water temperature in rivers : Ecological impacts and future resilience. 1–26 (2024) doi:10.1002/wat2.1724.
34. Snook, R. R., Bretman, A., Dougherty, L. R. & Fricke, C. The consequences of rising temperatures for animal fertility. *Nat. Rev. Biodivers.* **2**, 225–241 (2026).

Methods

Biodiversity data

Nesting sandbanks are of socio-ecological importance, and safeguarding them can co-benefit multiple species, from aquatic to terrestrial, as well as the local communities that depend on these ecosystems. Among the fauna, at least two species of Amazonian turtles are strictly dependent on those habitats for its reproduction: the Giant Amazonian River Turtle, *Podocnemis expansa*, which represents the largest South American freshwater chelonian; and the Six-tubercled Amazon River Turtle, *Podocnemis sextuberculata*, the smallest Podocnemididae and first to nest when sandbanks begin to emerge at the onset of the dry season[6]. The Yellow-spotted River Turtle, *Podocnemis unifilis*, also uses the sandbanks, but shows a more generalist nesting strategy, nesting in a broad range of habitats rather than relying exclusively on sandbanks[28].

As long-lived animals consumed by local people, turtles are excellent to model the potential socio-ecological impacts of climate change in Amazonia. Due to its large size, *Podocnemis expansa* was the main target and has a history of being harshly targeted by humans for its high protein value, with historical reports of declines across Amazonia[24]. Its drastic decline led to increasing exploitation and pressure on the smaller and congeneric species, *P. sextuberculata* and *P. unifilis*. Currently, all Podocnemidid species are categorized either as Vulnerable (VU) or Endangered (EN) by the International Union for Conservation of Nature Red List of Threatened Species[35].

Efforts to protect Amazonian turtle species date back to the late 70's. Stading as one of the most enduring and large-scale wildlife initiatives in the Brazilian Amazon, the Amazon Turtles Program (Programa Quelônios da Amazônia – PQA), was created in 1979 by the Brazilian Government, aiming to protect and recover the natural populations of Amazonian Turtles across the biome[36,37]. Hence, PQA was implemented as a conservation program that protects nesting turtles and sandbanks[37].

To date, PQA represents one of the main long-term wildlife conservation programs carried out by the Brazilian Institute of Environment and Renewable Natural Resources (IBAMA), formerly known as the Brazilian Institute for Forest Development (IBDF)[37]. Given limited funding and human resources, partnerships with local communities, NGOs, and municipality engagement have been critical to sustaining the program over the long-term and expanding its geographic reach[36,37]. In 2007, following

the division of the Brazilian Environmental Agency into IBAMA and the Chico Mendes Institute for Biodiversity Conservation (ICMBio), key sites within protected areas, such as the Abufari Biological Reserve (REBIO Abufari) and the Trombetas Biological Reserve (REBIO Trombetas), continued to be monitored under the responsibility of ICMBio[37]. Another example is the "Pé-de-pincha program", which since 1999 with support from the Federal University of Amazonas (UFAM), established the first community-based monitoring and management program for riverine turtles in partnership with the riverine communities of Terra Santa, in the lower Amazon, Amazonas State[4,6]. The data collected also follow the protocols established by IBAMA, yielding similar results. Decentralizing natural resource management through the involvement of local communities has proven effective in supporting biodiversity recovery and in shaping policies grounded in community-based management[5]. Since its creation, the "Pé-de-pincha" Program has been implemented in 123 communities across 18 municipalities in the states of Amazonas and Pará, with 56% of these located outside conservation units, thereby contributing to turtle protection beyond formally protected areas[4].

Despite some funding and logistical constraints, PQA has a long time-series of turtle nesting monitoring, which uses the same protocol in different nesting sites across Amazonia, allowing the monitoring of trends[6,37]. The quality of data varies throughout locations with gaps and variation of funding and support over the years, with *P. expansa* being the most representative species in the data[37]. While nest counts are feasible in some areas, in others the high density and overlap of digging and nesting throughout the season make accurate counts impractical[6,37]. In most areas, the only data available are the total number of hatchlings per season, which represent the most consistent and reliable data collected since the beginning of PQA[37].

Our analysis was based on the data available for *P. expansa* (Table 3), however, implications for the other congeneric species and the ecosystem were discussed. We defined a region of interested (ROI) within each study site based on the home range (HR) estimates for *P. expansa* with the monitored sandbanks at the centre of the ROI, which covered 1 up to 3 times the HR for the species (Linear Home Range [LHR] of 13 km and Autocorrelated Kernel Density Estimator [AKDE] up to 294 km^2; Souza et al. 2025). Therefore, Trombetas' ROI was 708.08 km^2 and length of 38.35 km, Purus

ROI measured 442.6 km^2 and the length was 62.41 km, and Tapajós ROI was 353 km^2 with 31 km length.

In-situ sand temperature

At Tapajós River, temperature records from in-situ dataloggers were compiled during the dry season of 2018 (n=13), 2019 (n=26), and 2024 (n=6). The devices (HOBO connect 2.3.0) were installed inside nests of *P. expansa* at Monte Cristo sandbar and monitored by IBAMA. It provided temperature, date and time for the monitoring period that consisted of 50 sampling days in 2018, 49 days in 2019, and 51 in 2024. For each datalogger, monthly summary statistics were calculated, and then a representative incubation temperature was estimated for each nest as the daily median temperatures recorded throughout the monitoring period. The proportion of female hatchlings expected from each nest was estimated using a Hill equation relating incubation temperature to sex-ratio.

Comparisons between in situ and satellite-derived temperatures focused on the Early Morning and Morning datalogger measurements, as Landsat overpasses occurres during the late morning period and were therefore expected to correspond most closely to temperatures recorded at those times. Overpass times varied slightly among study regions, occurring at approximately 10:20a.m. at the study site in Tapajós River (Path 228 and Row 063). For each matching window, we calculated the median temperature difference (bias) between methods; the overall disagreement between methods using Root Mean Square Error (RMSE); and Pearson correlation coefficient. To improve the spatial correspondence between satellite-derived temperatures and in-situ measurements, we also obtained satellite temperature extraction restricted to the portion of the target sandbank where dataloggers were deployed, rather than calculating temperature statistics across the entire sandbank surface within the ROI. This approach was adopted to minimize spatial mismatch between the two measurement methods.

In-situ water temperature

Water temperature is a readily measurable variable and has been extensively collected in a variety of contexts, particularly through routine monitoring and surveillance programs for water resource management[38]. In Brazil, the Brazilian National Water

Agency (Agência Nacional de Águas e Saneamento Básico - ANA) provides daily altimetric data on rivers water levels, flow rates, water temperature, and rainfall across the country. Some stations date back to the 1930's, providing a broad view of temporal trends; however, they are derived from infrequent monitoring for much of the record, with sampling frequency increasing from the mid-1990s onwards. To obtain and identify temporal trends on water temperature we retrieved hydrological data from Hidroweb (HW; https://www.snirh.gov.br/hidroweb/) from 1998 to 2024, when available, for each station, as water temperature is not consistently recorded every month or at every station. To allow comparison, we considered only data for the receding and dry season (September to December), when sandbanks are visible. We used data from 1998 onwards, which correspond to the period when it was collected more frequently.

Along the Purus River, the stations (N = 11) had a minimal of 297.23 km (Arumã station to Abufari) to the study area, following the river course. In the Trombetas River, there was one station right in the study area (Tabuleiro – REBio Trombetas) and others with distances varying from 30 (N = 6). And at Tapajós, the nearest station was 88 m to the monitored nesting site (N = 7).

Data is shown as three temperature measurements per day, which also included time of collection. We examined the data to obtain a mean, median, maximum, and minimum temperature per period of the day (e.g. morning, afternoon). Evening values were rare, and, therefore, not considered. We examined trends in the data per time of the say (morning and afternoon).

We also used the Hidroweb (HW) data to obtain the river elevation and the peak of dry season at each year for each study site defined by the lowest river level. These dates were used as guides to obtain satellite imagery of the sandbanks on the driest period of the year, therefore, when they are larger and most visible due to the high spectral contrast between water and exposed beaches. In many cases, when images were unavailable or of poor quality, we used the best available image for the dry season of that period (September to December). Data on river levels is available for more stations than data on temperature. In this case, for the Purus River, we obtained

data from 24 stations, and for the Trombetas, from 23 stations, and Tapajos, there were data available from 18 stations.

Satellite data processing

We employed the cloud-based platform Google Earth Engine (GEE) to process Landsat imagery (Landsat missions 5, 7, 8, and 9 Collection 2 Level-2 Surface Reflectance) between 1998 and 2024 from the falling to the low water season (September to December), when sandbanks stand out due to the contrasting spectral reflectance between the water and the beaches. For that, we filtered images by date (01 September to 01 January of the following year, since GEE is exclusive and uses zero-based day counting). We restricted to scenes with reported scene-level cloud cover < 25% or the least cloudy scene for that drought period (minimum CLOUD_COVER in GEE). We also removed cloud-contaminated pixels using the QA_PIXEL bitmask in GEE, which produces a conservative mask to avoid biased temperature estimates due to clouds. The Landsat product identifier (Landsat ID) was retained as metadata. All images were clipped to our ROI.

We developed three GEE workflows to extract per-pixel surface temperature and spatial covariates from Landsat (C2 L2) scenes: two to extract Water Surface Temperature (WST) and one for sandbanks (LST).

Firstly, water bodies were identified using the Normalized Difference Water Index (NDWI), calculated from the green and near-infrared bands, as follows:

$$NDWI = \frac{Green - NIR}{Green + NIR}$$

where:

- Green: Landsat 5/7, band SR_B2 (0.52–0.60 μm); Landsat 8/9, band SR_B3 (0.53–0.59 μm).
- Near Infrared (NIR): Landsat 5/7, band SR_B4 (0.76–0.90 μm); Landsat 8/9, band SR_B5 (0.85–0.88 μm)[39].

To mask the sandbanks, we used the Shortwave Infrared 1 (SWIR1): Landsat 5/7, band SR_B5 (1.55–1.75 μm); Landsat 8/9, band SR_B6 (1.57–1.65 μm).

Hidroweb approach using Landsat (satellite)

1. to simulate the Hidroweb approach, we obtained WST from randomly selected sampling locations. In this method, to capture spatial variability while preserving randomization, the ROI was subdivided into three equal-width zones aligned with the river reach (longitudinal for Purus and Tapajós; and transversal for Trombetas). A water centerline proxy was derived by identifying local maxima ("ridge" pixels) of the distance-to-edge within the water mask using a 3×3 neighborhood. We defined a sampling window of a 300 m buffer around the centerline, constrained to the 'safe-water' region, defined as 180 m from the river edge. Three random candidate points were selected from each zone within the ROI (nine points per scene) and used to extract WST from pixels classified as water within the safe-water and from each zone of the ROI. In this method, lakes, oxbow lakes, and connectivity within the ROI could be considered at random. The resulting time-series contains WST estimates collected for each Landsat scene available during the dry season (September to December) of each year between 1998 and 2024.

All pixels masked as Water (WST)

2. The second method to obtain the WST consisted of extracting the temperature of all pixels masked as water in each Landsat scene; however, the analysis was constrained to a buffer clipped around the river centerline in the main channel. Therefore, for this method, lakes, oxbow lakes, or other connective features were excluded. The centerline buffer sized varied for each study area based on the river width, using the RivWidthCloud Algorithm[40]. To minimize mixed pixels near banks and shallow margins, a distance-to-edge metric was calculated using a fast Euclidean distance transform. Only pixels located at least 90 m from the riverbank were retained.

All exposed sand pixels (LST)

3. the sand pixels were delineated and masked using a brightness threshold on SWIR1 reflectance. To ensure that only exposed sandbanks were retained, all pixels classified as water were excluded. The resulting sandbank mask represents all exposed sand pixels within the buffer (clipped to the main

channel). The LST sampling was then obtained for all sand pixels present in each Landsat scene clipped to the centerline buffer.

In all methods, W/LST was derived from Landsat C2-L2 products acquired by the Thematic Mapper (TM; Landsat 5; 120 m resolution), Enhanced Thematic Mapper Plus (ETM+; Landsat 7; 60 m resolution), and Operational Land Imager/Thermal Infrared Sensor (OLI/TIRS; Landsat 8 and 9; 100 m resolution) [41–44]. Surface temperature was obtained from the USGS-provided Surface Temperature (ST) band, which is atmospherically corrected and distributed in scaled integer format. The ST_B6 band was used for Landsat 5 and 7, and ST_B10 for Landsat 8 and 9. Each thermal band was converted to surface temperature following the scale and offset factors provided in the Landsat metadata. The final W/LST temperature datasets were resampled to the original Landsat thermal band resolution. The digital numbers were converted to temperature in Kelvin using the product-specific scaling factor and additive offset and subsequently converted to degrees Celsius for analysis. The USGS C2-L2 Surface Temperature (ST) product, incorporates atmospheric correction and emissivity estimation during USGS processing[45]. These data provided continuous, consistent measurements of Earth's surface temperature across diverse landscapes to support long-term environmental studies. Additionally, quality flags and uncertainty metrics provide a framework for filtering and analysing data based on their reliability, so that data may be absent for a given region if it does not meet the reliability criteria.

For each scene, we also obtained the water-surface extent and the exposed sandbank area within the main channel. This was obtained by summing the pixel areas of all sandbank pixels within the clipped buffered ROI. Area estimates were reported in square kilometres (km²).

Estimation of annual hatchling sex-ratios

Annual hatchling sex-ratios were estimated based on the annual sand thermal pattern and the total number of live hatchlings produced per year in each study site, using the Hill equation (adapted by Laloë et al. 2014[18]) as follows:

$$sr(t) = \frac{1}{1+e(1/S)(\ln(P+K)-\ln(t+K))}$$

where sr(t) is the predicted proportion of females, *P* is the pivotal temperature (32.6°C, for the target species), *S* controls the slope of the response curve (S= 0.0336281), and *K* is a is a small constant (K=0.1), so that lower temperatures produced males and higher temperatures produced females.

Only temperature data from October onwards were included in the sex-ratio estimates to correspond to the expected period of gonadal differentiation (25 to 35 days of incubation). Temperature classes below 28°C and above 40°C were treated as lethal, however, because hatchling totals represented individuals that had already survived to hatching, mortality was not applied directly to the hatchling counts. Instead, mortality thresholds were used to exclude lethal temperature classes, then live hatchlings were redistributed among viable temperature classes. Therefore, only the remaining viable temperature classes were retained for sex-ratio estimation.

Matchups

Same-day and nearest-date matching procedures were implemented between in-situ (water and sand data) and satellite datasets. Each matched pair was assigned to the smallest tolerance window, using the following categories: ±3 days, ±5 days, ±10 days, ±15 days, and over 15 days. WST and LST satellite data were kept as a matchup for all scenes. To ensure consistent support for comparisons, temperatures were aggregated to median, maximum and minimum values per day for each dataset. Temperatures were compared using matched pairs. The agreement between satellite-derived and in-situ (HW) temperatures was evaluated using paired observations matched within temporal windows ranging from the same day to ±15 days. Pearson's correlation coefficient (r) was used to assess the strength of the linear association between datasets, while paired t-tests were used to determine whether the mean temperature difference differed significantly from zero. Model performance was further quantified using the Root Mean Square Error (RMSE), which measures the average deviation between dataloggers temperatures, with smaller RMSE values indicating closer agreement. To account for uncertainties, differences between in-situ sand temperature and satellite-derived were used to inform a sensitivity analysis of predicted hatchlings sex-ratios. For that, we developed scenarios representing the observed temperature differences as follow: Scenario1 = original satellite data;

Scenario2 = -2ºC; Scenario2: -3ºC; and Scenario4: -4ºC. Scenario3 was considered as the intermediate scenario.

Statistical analysis

Temporal trends in all timeseries were assessed using the Mann–Kendall test. Relationships between variables were evaluated using both Pearson and Spearman correlation coefficients, depending on data distribution and assumptions. To examine changes in the distribution of temperature classes over time, a Pearson's χ^2 test of independence was applied to contingency tables of Year × Temperature class counts. The strength of the association between year and the temperature-class distribution was quantified using Cramér's V, which ranges from 0 (no association) to 1 (complete association), providing a standardized measure of the magnitude of temporal variation in temperature-class composition. To visualize the overall temporal pattern in water temperature across all datasets we used the non-parametric method of Locally Estimated Scatterplot Smoothing (LOESS). Median annual temperature observations were plotted against sampling date, and a LOESS curve (span = 0.75) with 95% confidence intervals was fitted to each dataset separately to highlight underlying temporal trends while reducing the influence of short-term variability. Given the short-term fluctuations and extreme values, we used median temperature values as the representative thermal metric. All statistical analyses and tests were conducted in R 4.6.0 Core Team (2026).

Ethics. This article did not require am ethical assessment before being conducted.

Data availability

All Landsat data used for this assessment are publicly available. Hydrological data from Hidroweb can be assessed at: http://hidroweb.ana.gov.br. Turtle nesting data referent to REBIO Trombetas and REBIO Abufari were obtained after license approval (SISBio license number: 97540-1) and direct communication with IBAMA and ICMBio.

References

35. TTWG et al. Turtles of the World: Annotated Checklist and Atlas of Taxonomy, Synonymy, Distribution, and Conservation Status (10th Ed.). Conservation Biology of Freshwater Turtles and Tortoises: A compilation project of the IUCN SSC Tortoise and Freshwater Turtle Specialist Group. vol. 10 (Chelonian Research Foundation and Turtle Conservancy, California, USA, 2025).
36. Eisemberg, C. C., Vogt, R. C., Balestra, R. A. M., Reynolds, S. J. & Christian, K. A. Don't put all your eggs in one basket – Lessons learned from the largest-scale and longest-term wildlife conservation program in the Amazon Basin. *Biological Conservation.* 238, 108182 (2019).
37. Lacava, R. V. *et al.* Recovery of the Giant South American River Turtle in four decades of a network-based conservation program in the Brazilian Amazon. *Biodivers. Conserv.* 283–297 (2024)
38. Webb, B. W. Trends in stream and river temperature. *Hydrol. Process.* 10, 205–226 (1996).
39. McFEETERS, S. K. The use of the Normalized Difference Water Index (NDWI) in the delineation of open water features. International Journal of Remote Sensing, 17(7), 1425–1432, (1996).
40. Yang, X., Pavelsky, T. M., Allen, G. H. & Donchyts, G. RivWidthCloud: An Automated Google Earth Engine Algorithm for River Width Extraction from Remotely Sensed Imagery. *IEEE Geosci. Remote Sens. Lett.* **17**, 217–221 (2020).
41. Simon, R. N., Tormos, T. & Danis, P. Retrieving water surface temperature from archive LANDSAT thermal infrared data : Application of the mono-channel atmospheric correction algorithm over two freshwater reservoirs. *Int. J. Appl. Earth Obs. Geoinf.* **30**, 247–250 (2014).

42. Malakar, N. K. *et al.* An Operational Land Surface Temperature Product for Landsat Thermal Data : Methodology and Validation. *IEEE Trans. Geosci. Remote Sens.* **56**, 5717–5735 (2018).
43. Largier, J. L. High-Resolution Nearshore Sea Surface Temperature from Calibrated Landsat Brightness Data. (2024).
44. Vanhellemont, Q. Remote Sensing of Environment Automated water surface temperature retrieval from Landsat 8 / TIRS. *Remote Sens. Environ.* **237**, 111518 (2020).
45. Hulley, G. C., Malakar, N. K. & Freepartner, R. J. NASA ' s MODIS and VIIRS Land Surface Temperature and Emissivity Products : A Long-Term and Consistent Earth System Data Record. **11**, 522–535 (2018).

Code availability

The code needed to reproduce the results and figures presented in this study are available from the corresponding author on reasonable request.

Acknowledgements

The authors kindly thank IBAMA, ICMBio and local communities volunteers for all their effort during these years of protecting and monitoring the nesting sites of turtles. We are thankful to ICMBio for providing data on the monitoring of the REBio do Rio Trombetas and REBio Abufari. We acknowledge the 'Hydrology Bristol', at the School of Geographical Sciences, University of Bristol (UoB), UK, for their infrastructure support. We are also grateful to the Cabot Institute for providing opportunity for SF and other colleagues from UoB to gain GEE coding skills and participate in one-to-one sessions with Dr Cristiano Almeida, from the Federal University of Paraíba (UFPB). We are sincerely grateful to both the Cabot Institute for facilitating this opportunity and to Dr Almeida for his generous support and expertise. We also would like to thank Dr Cinthia Maria Abreu Claudino from UFPB for the help with the timeseries analysis and reviewing GEE errors. We acknowledge the support from MSc Ali Hasnain, University of Punjab, with the help with GEE coding and areas estimations. And Dr Lidiane Gouvea for her thoughtful feedback on writing and style. This project was under a SISBio license (Number: 97540-1). SF is a Daphne Jackson Fellow funded by the Natural Environment Research Council (NERC), UK. Dr Ayan Fleischmann thanks the financial support by the Royal Society International Science Partnerships Fund International Collaboration Award (no. ICAO/R1/241102).

Author contributions
S.F. and R.B.N. conceptualized the work. The methodology was developed by S.F. with input from all co-authors during regular discussions. In-situ nesting data was collected annually by volunteers from local communities across Amazonia with support from R.V.L., R.A.F. and P.M.A. The original draft was written by S.F. with subsequent review and edits from all co-authors.

Competing interests
The authors declare no competing interests.

Additional information

Correspondence and requests for materials should be addressed to Shirley Famelli.

Tables and Figures

Table 1. Water temperature trends across the datasets and study areas. *shows where Mann-Kendall trends were significative ($p < 0.05$). In-situ water temperature was collected by Hidroweb, satellite (random points), WST: Water Surface Temperature; LST: Sand Surface temperature.

Study area	Dataset	Mann-Kendall trend	Sen's slope	95% Confidence Interval	p value
Purus	in-situ	0.281	0.05	0–0.104	0.04*
	satellite	0.287	0.23	0.0106–0.408	0.04*
	WST	0.355	0.25	0.0658–0.436	0.01*
	LST	0.275	0.3	0.006–0.4993	0.05*
Trombetas	in-situ	0.211	0.07	-0.0280–0.146	0.194
	satellite	0.249	0.10	-0.0138–0.246	0.07
	WST	0.298	0.13	0.00788–0.272	0.03*
	LST	0.16	0.04	0.011–0.079	0.0096
Tapajós	in-situ	0.457	0.17	0.0659–0.264	0.003*
	satellite	0.413	0.16	0.0463–0.299	0.003*
	WST	0.403	0.18	0.0604–0.323	0.004*
	LST	0.286		0.001–0.268	0.043

Table 2. Temporal variation in the Water Surface Temperature (WST) and Land/Sand Surface Temperature (LST) across years in the study areas across the timeseries (1998 to 2024). Pearson's χ^2 tests whether an association exists and Cramér's V tells how strong that association is (0 = no association, closer to 1 = stronger association).

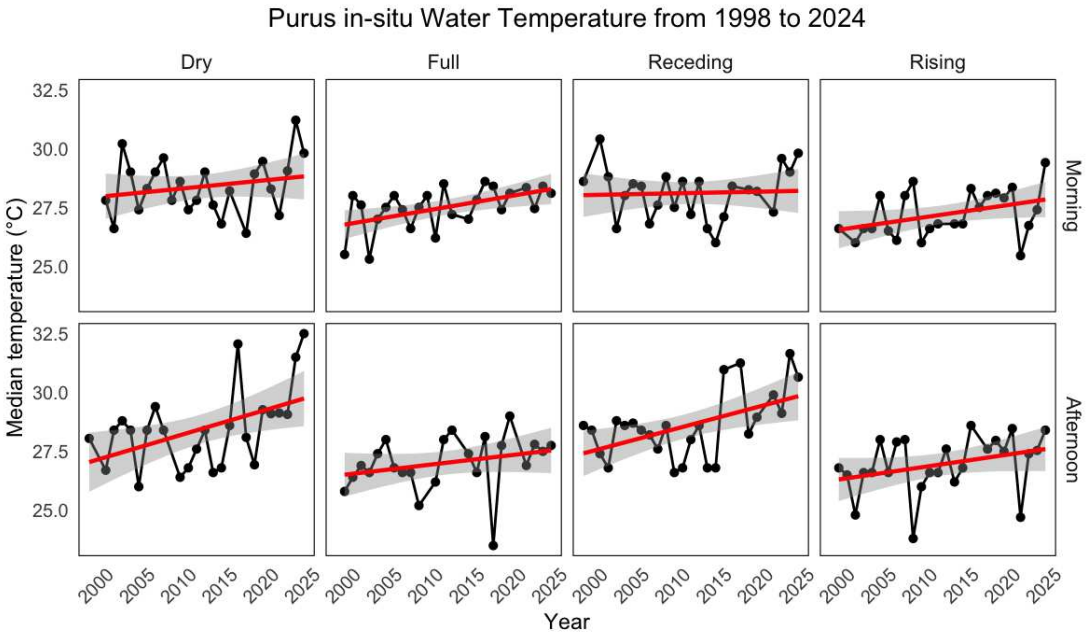
Study site	**χ^2**	**p**	**Cramér's V**
Purus WST	275,171	$p < 0.001$	0.499
Purus LST	10,144	$p < 0.001$	0.49
Trombetas WST	163,082	$p < 0.001$	0.284
Trombetas LST	15,011	$p < 0.001$	0.39
Tapajós WST	413,674	$p < 0.001$	0.341
Tapajós LST	44,564	$p < 0.001$	0.26

Table 3. Life-traits, natural history parameters, and ecological temperature classes for embryonic development of the Podocnemidid turtles in Amazonia.

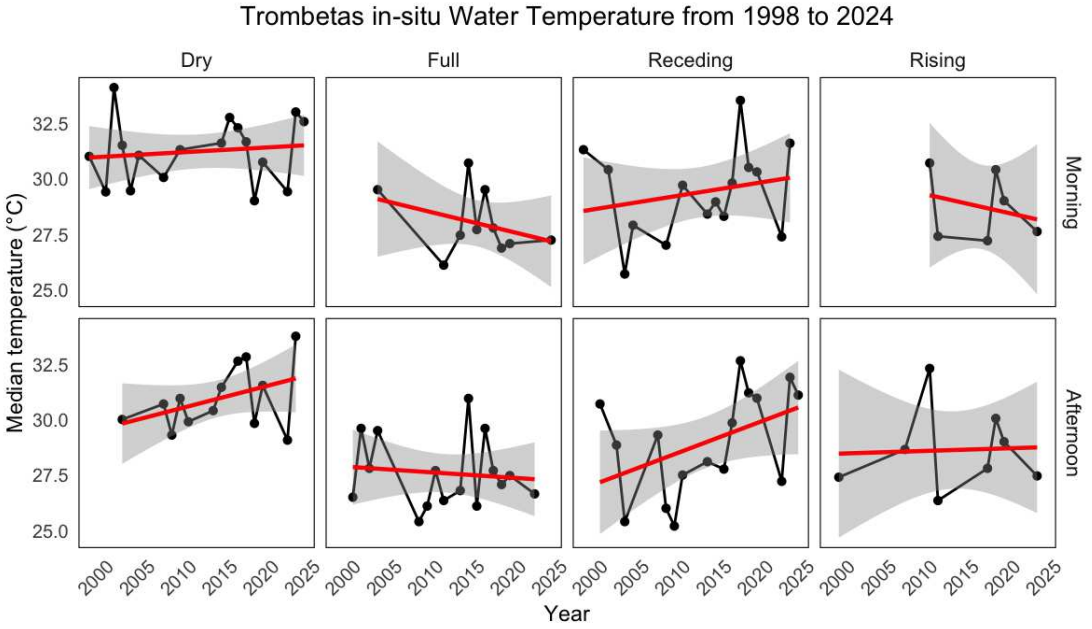
Parameter	**Values**	**Reference**
Incubation period of *P. expansa*	58 days	[22]
Gonads differentiate	around days 25-35 of incubation	[19]
Clutch size (varies upon female size and geography)	18 to 189 eggs	[28]
Clutch frequency	Each adult female nest only once per dry season	[28]
Survival threshold	<28°C	[19]
Male development	28–31°C	[19]
pivotal temperature, (produces 1:1 sex-ratios)	32.6°C	[19]
survival threshold in lab conditions for *Podocnemis sextuberculata*	38°C	[21]
survival threshold in the wild (embryos might survive temperature fluctuations when not prolonged)	40°C	[19]
Sexual maturity in *P. expansa*	5–10 years 15–17 years	[20]

Figures:

a


Purus in-situ Water Temperature from 1998 to 2024
Dry
Full
Receding
Rising
Morning
Afternoon
Median temperature (°C)
32.5
30.0
27.5
25.0
2000
2005
2010
2015
2020
2025
Year

b


Trombetas in-situ Water Temperature from 1998 to 2024
Dry
Full
Receding
Rising
Morning
Afternoon
Median temperature (°C)
32.5
30.0
27.5
25.0
2000
2005
2010
2015
2020
2025
Year

c

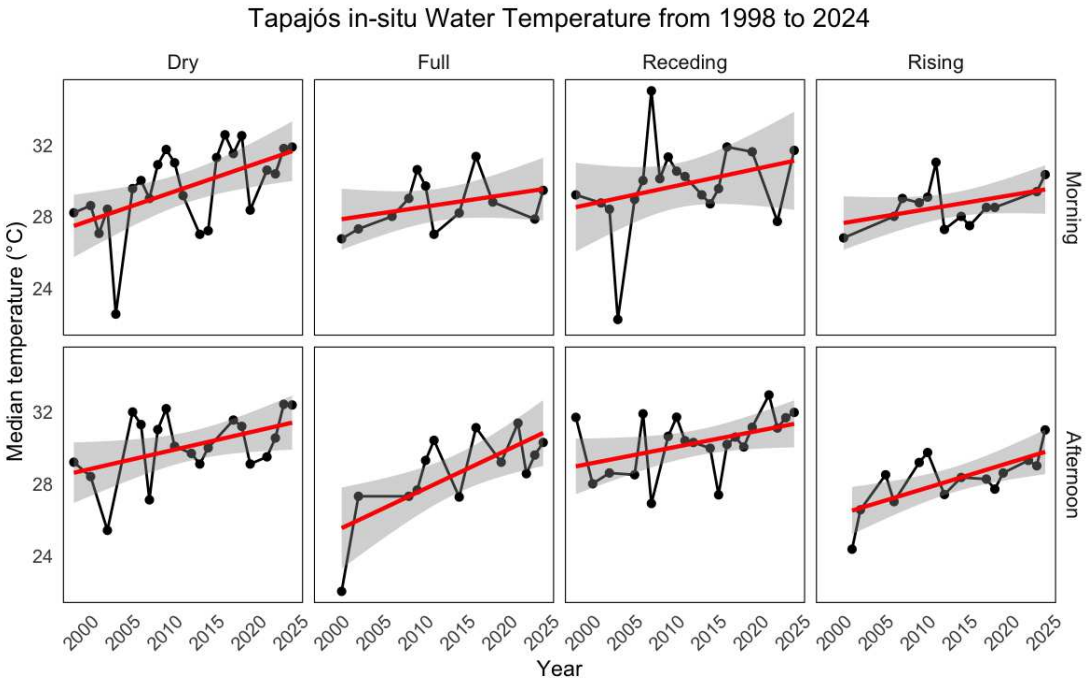
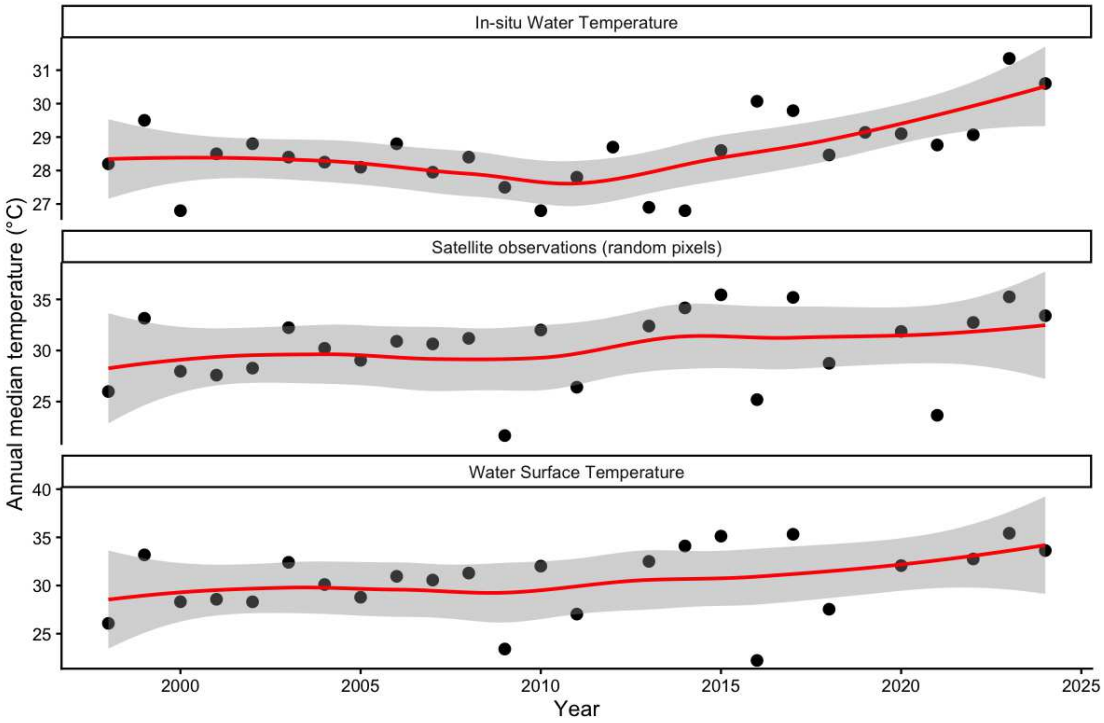


Fig. 2 | In-situ water temperature collected by Hidroweb along the selected study areas: a) Purus, b) Trombetas, c) Tapajós rivers, from 1998 to 2024. Results are presented as median values per season.

a



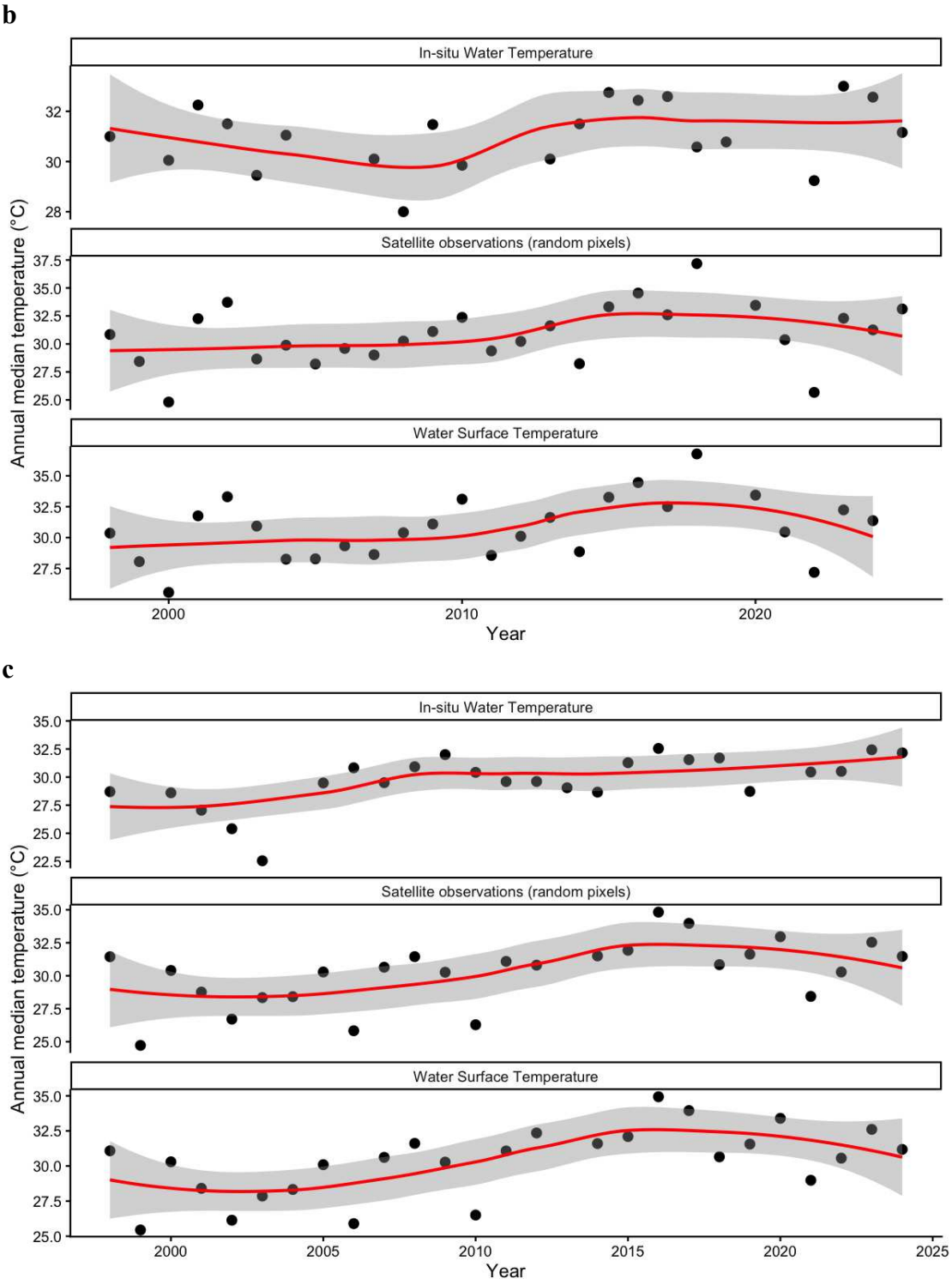
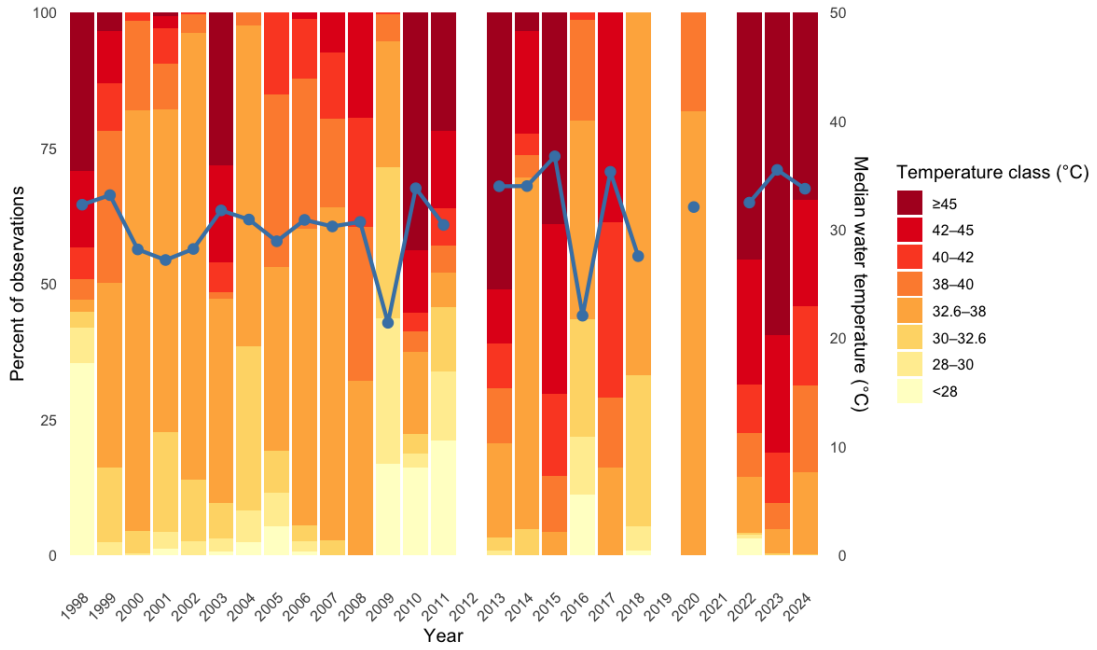
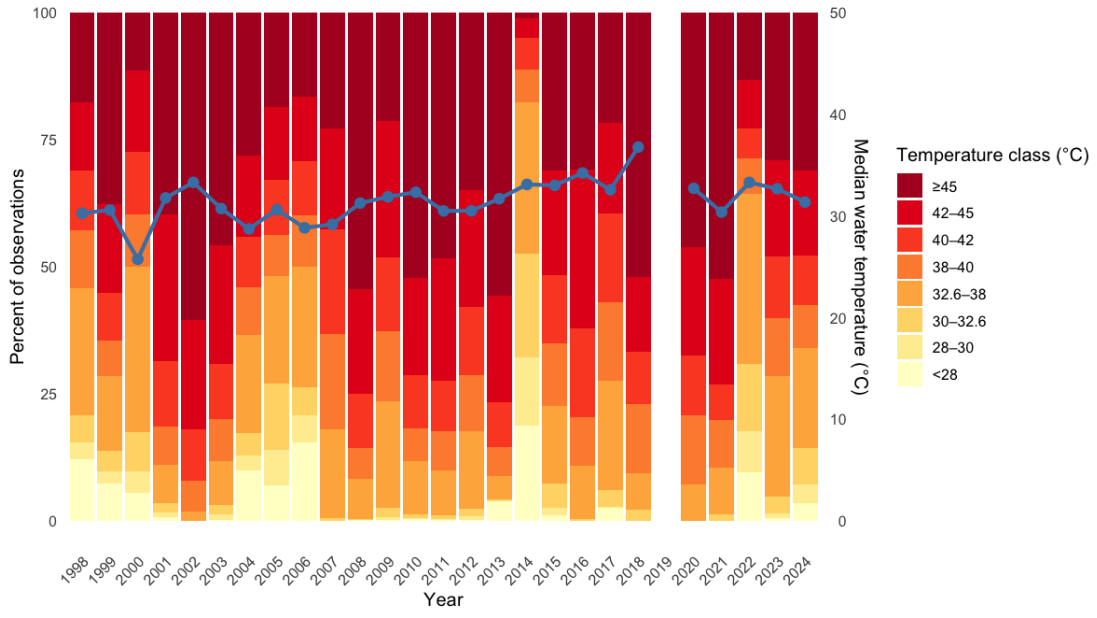


Fig. 3 | Temporal variation in annual median water temperature across all datasets. The red line represents a locally estimated scatterplot smoothing (LOESS) curve fitted to the annual median values, with shaded areas indicating 95% confidence intervals.

a


Percent of observations
Median water temperature (°C)
Year
Temperature class (°C)
≥45
42–45
40–42
38–40
32.6–38
30–32.6
28–30
<28

b


Percent of observations
Median water temperature (°C)
Year
Temperature class (°C)
≥45
42–45
40–42
38–40
32.6–38
30–32.6
28–30
<28

c

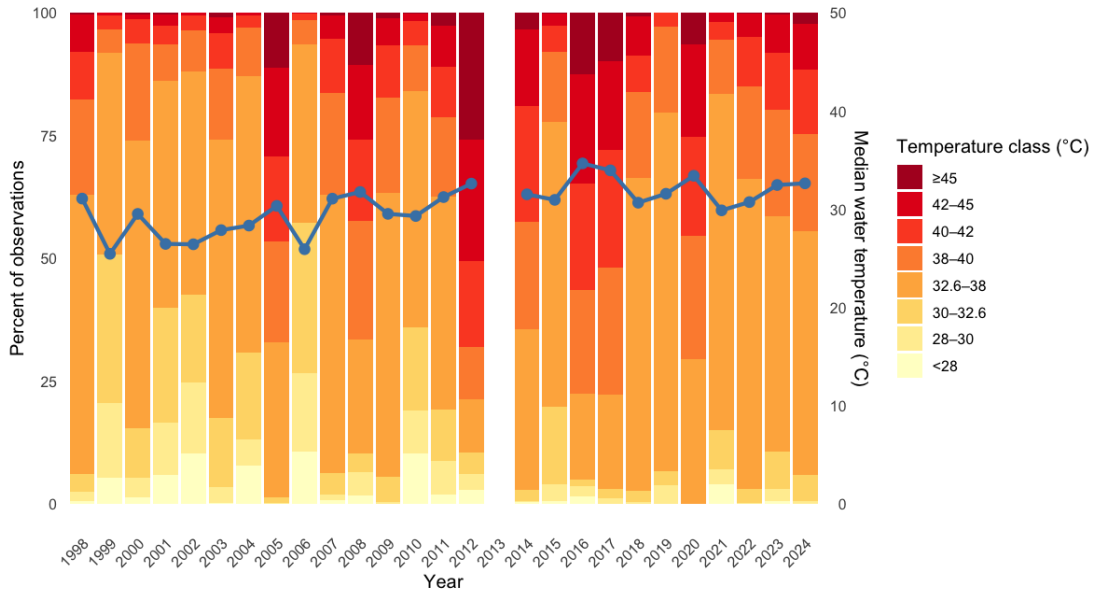
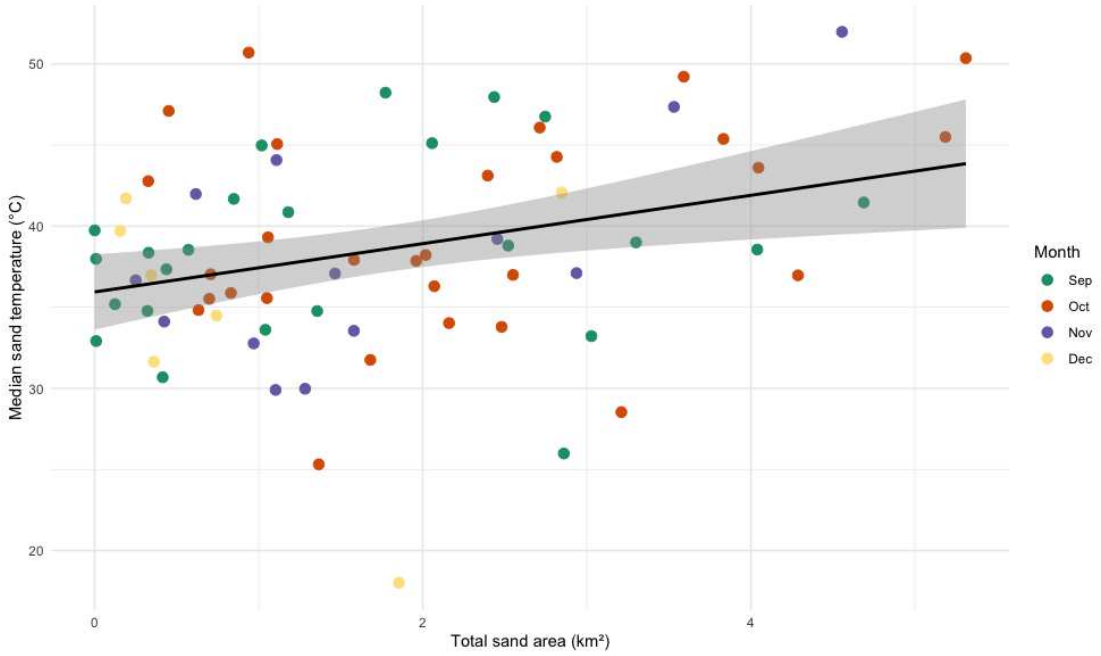


Fig. 4 | Annual thermal pattern of water (line) and sandbanks (bars) at the (a) Purus, (b) Trombetas, and (c) Tapajós Rivers. Water temperature is shown as median value per year, and sand temperature shows data accumulated from September to December 1998 to 2024.

a



b

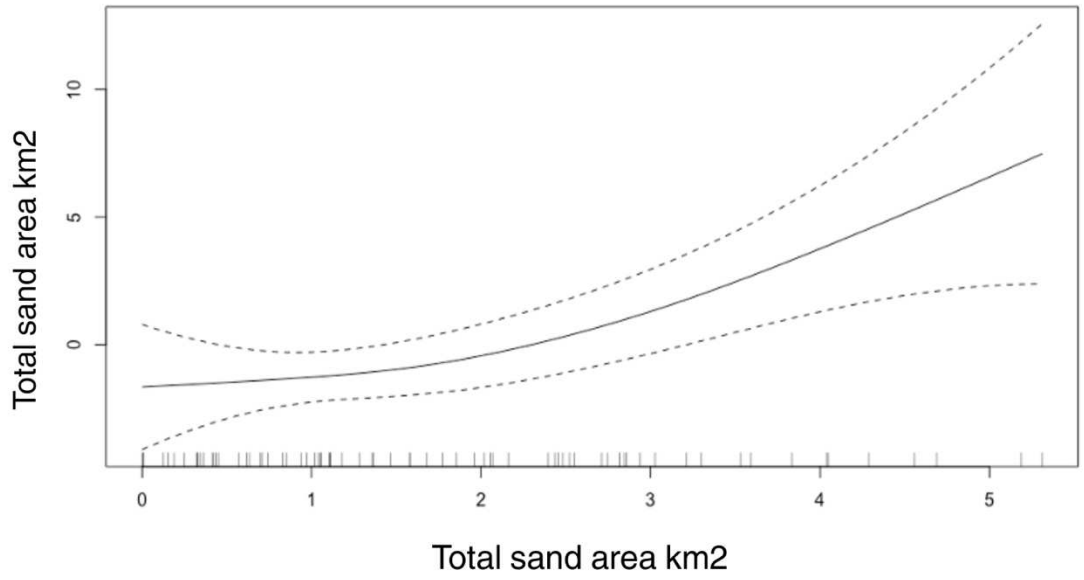
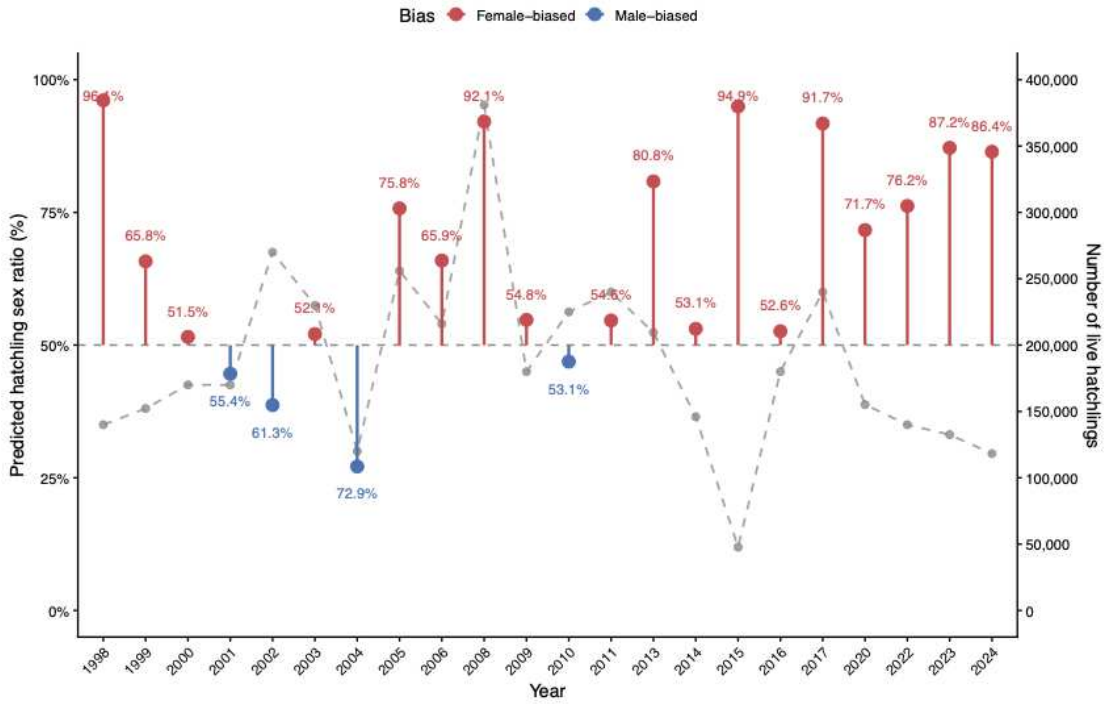
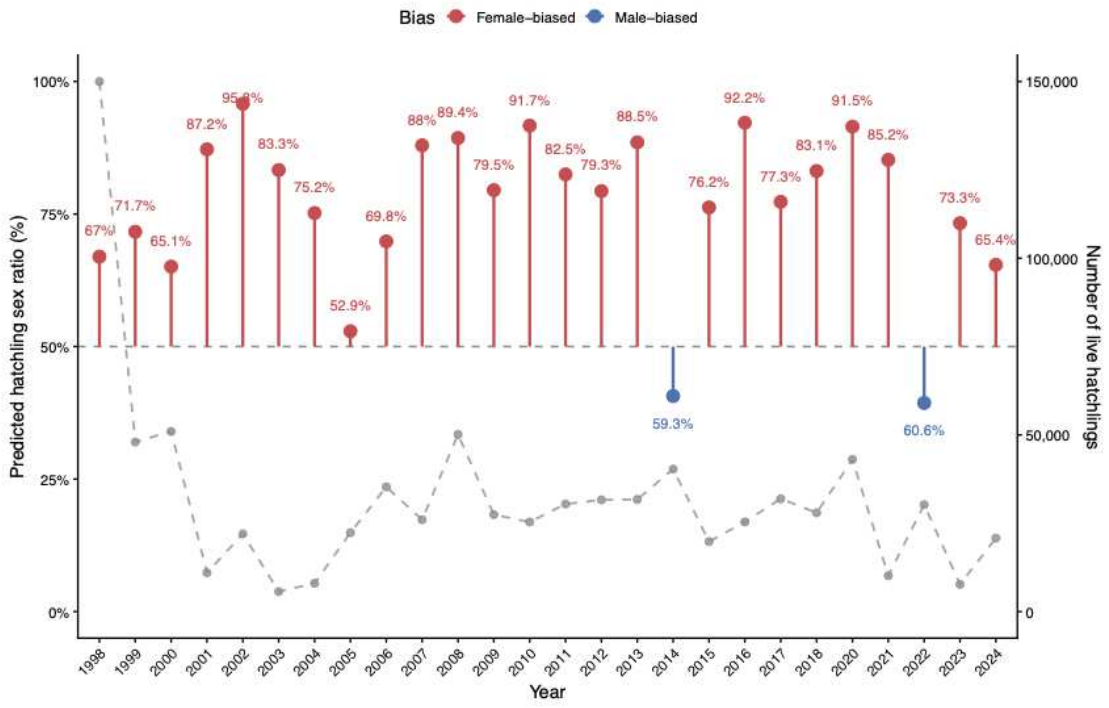


Fig. 5 | **a)** Fitted linear trend relationship between total exposed sand area and median sand temperature across Landsat scenes at Abufari Biological Reserve, Purus river. Points are coloured to indicate the month (September–December). **b**) Generalized additive model (GAM) illustrating the nonlinear relationship between total sand area and median sand temperature at Purus river, Abufari Biological Reserve (REBio Abufari), with shaded 95% confidence intervals.

a



b



c

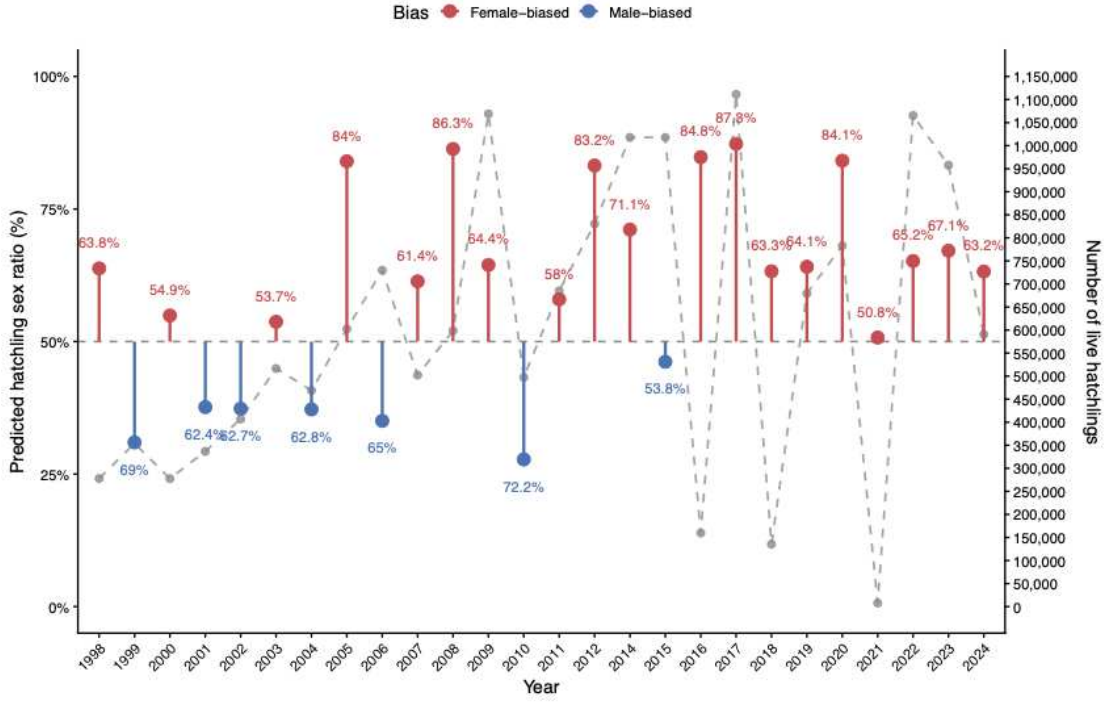
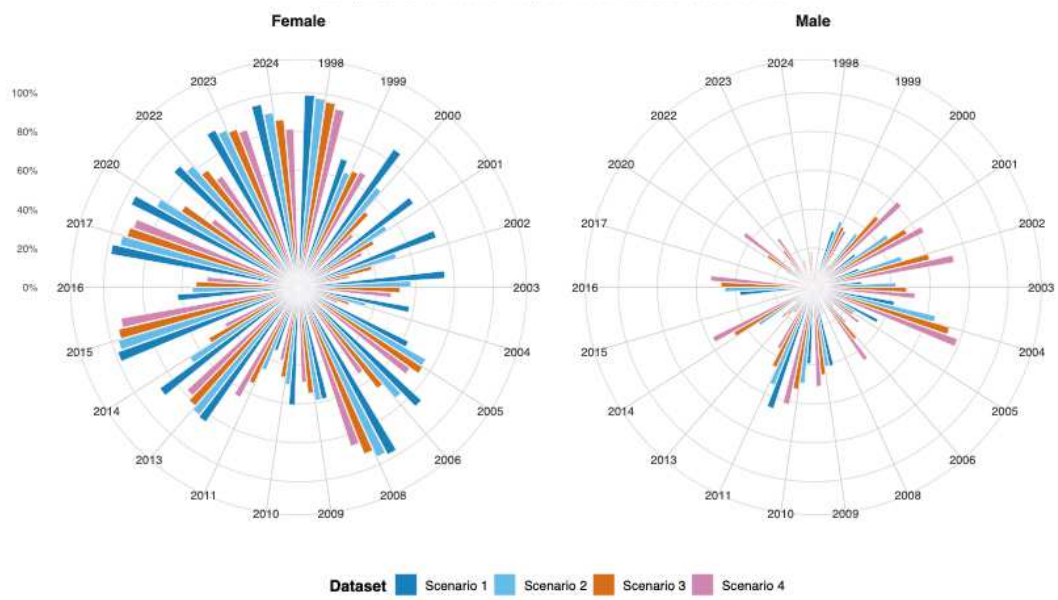


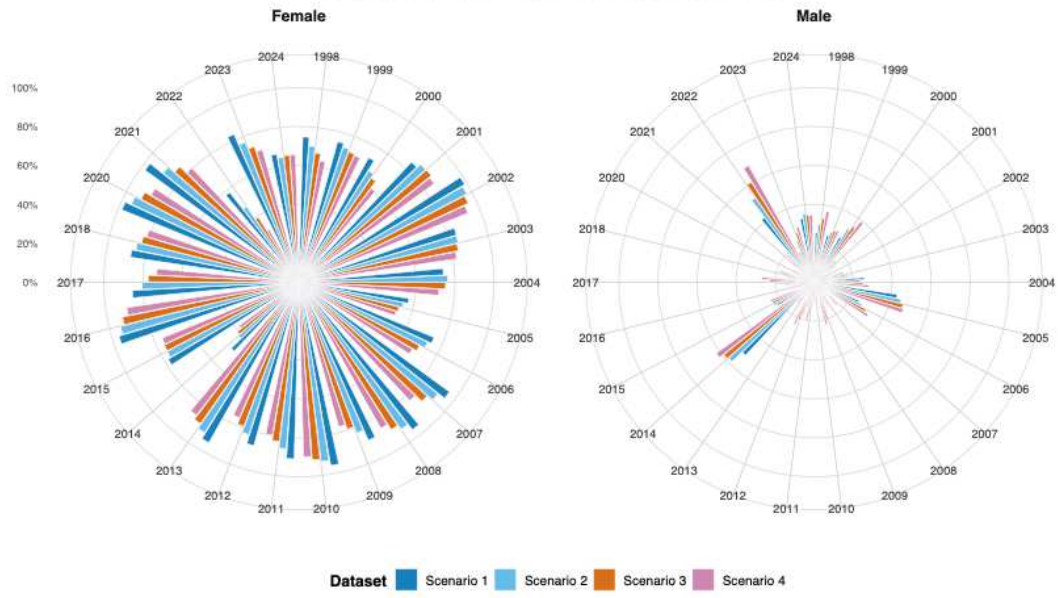
Fig. 6 | Sex-ratio estimation based on the thermal profile of sandbars collected with Landsat observation between October and December 1998 to 2024. Data is shown

after corrections (Scenario3) at (a) Abufari Biological Reserve, Purus River; (b) Trombetas Biological Reserve, Trombetas River; and in the (c) Monte Cristo sandbar at Tapajós River.

a



b



c

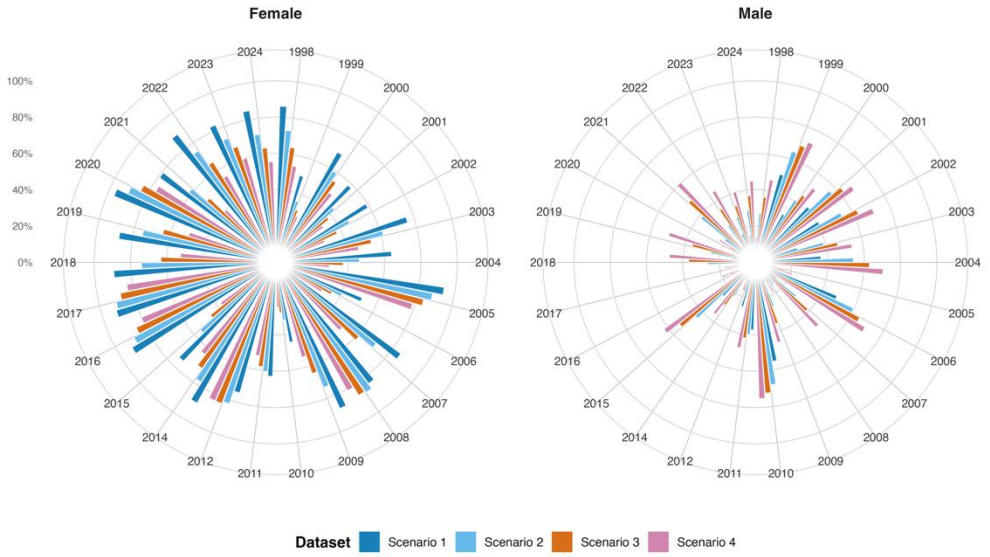


Fig. 7 | Sensitivity test showing the comparison of female and male predictions across four model scenarios (Scenario1: original satellite data; Scenario2: -2ºC; Scenario3: -3ºC; Scenario4: -4ºC) from between October and December 1998 to 2024 at (a) Abufari Biological Reserve, Purus River; (b) Trombetas Biological Reserve, Trombetas River; and in the (c) Monte Cristo beach at Tapajós River.

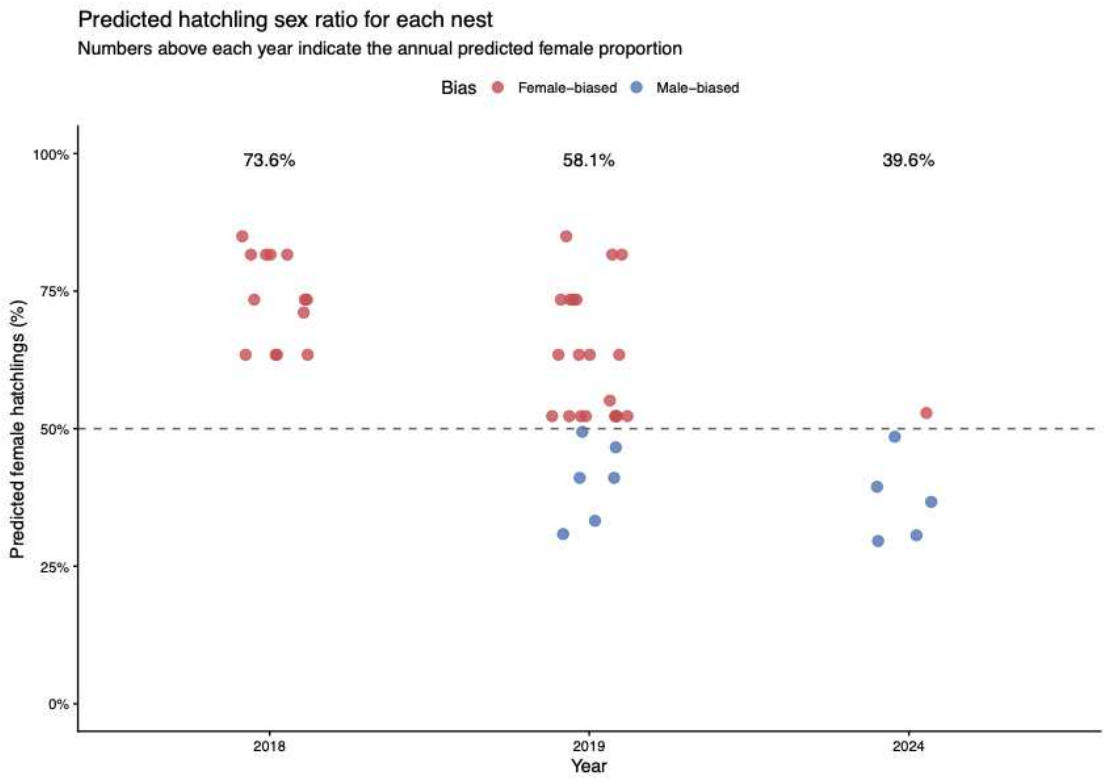


Fig. 8 | Sex-ratio estimation based nesting monitoring with dataloggers at Monte Cristo beach, Tapajós River, Pará. Percentage refers to the amount of females estimated.

Supplementary Files

This is a list of supplementary files associated with this preprint. Click to download.

- SupplementarymaterialFamellietal..docx